JACS
JOURNAL OF THE AMERICAN CHEMICAL SOCIETY

Communication

pubs.acs.org/JACS

# Measurement of Active Site Ionization Equilibria in the 670 kDa Proteasome Core Particle Using Methyl-TROSY NMR

Algirdas Velyvis*,† and Lewis E. Kay*,†,‡

†Departments of Molecular Genetics, Biochemistry, and Chemistry, University of Toronto, Toronto, Ontario, Canada M5S 1A8

‡Program in Molecular Structure and Function, Hospital for Sick Children, 555 University Avenue, Toronto, Ontario, Canada, M5G 1X8

Supporting Information

**ABSTRACT:** The 20S proteasome core particle is a molecular machine that plays a central role in the regulation of cellular function through proteolysis, and it has emerged as a valuable drug target for certain classes of cancers. Central to the development of new and potent pharmaceuticals is an understanding of the mechanism by which the proteasome cleaves substrates. A number of high-resolution structures of the 20S proteasome with and without inhibitors have emerged that provide insight into the chemistry of peptide bond cleavage and establish the role of Thr1 O$\gamma$1 as the catalytic nucleophile. The source of the base that accepts the Thr1 H$\gamma$1 is less clear. Using a highly deuterated sample of the proteasome labeled with $^{13}CH_3$ at the Thr-$\gamma$ positions, the p$K_A$ of the Thr1 amino group has been measured to be 6.3 and hence deprotonated in the range of maximal enzyme activity. This provides strong evidence that the terminal amino group of Thr1 serves as the base in the first step of the peptide bond cleavage reaction.

The 20S proteasome core particle (CP) is a 670 kDa barrel-like structure that regulates cellular homeostasis by degrading misfolded or damaged proteins before they accumulate to levels that would interfere with cell function.[1] It consists of four heptameric rings that are stacked on top of each other[2] as $\alpha_7\beta_7\beta_7\alpha_7$, Figure 1A. In the case of the 20S CP from the archaeon *Thermoplasma acidophilum*, each of the heptamers is comprised of seven identical repeats of a single polypeptide chain, either $\alpha$ or $\beta$, that simplifies structural studies relative to eukaryotic versions of the molecule where seven distinct $\alpha$ and $\beta$ subunits are used. Active-site residues that catalyze the degradation of substrate polypeptides are localized to the $\beta$ subunits and are sequestered in the lumen of the 20S CP barrel.[3] Key residues include Thr1, Lys33, Glu17, and Asp166, Figure 1A, with mutation of any of these amino acids abrogating activity. Structures of the 20S CP with bound covalent inhibitors unequivocally establish that the hydroxyl oxygen of Thr1 is the catalytic nucleophile.[3,4] The identity of the base that accepts the hydrogen ion from the Thr1 hydroxyl moiety is less clear, however, since amino groups of both Thr1 and Lys33 (N$\zeta$) emerge as candidates due to their proximity to Thr1 O$\gamma$1. It is unlikely, however, that Lys33 is the catalytic base since it would be expected to be fully protonated in the pH interval 6–9, where a broad pH optimum activity profile is observed.[5] If the amino group of Thr1 is the base, then it must be deprotonated at the initial stage of the hydrolysis reaction. In principle, this can be tested by measuring the p$K_A$ of the amino-terminal group using solution NMR spectroscopy. Indeed, studies of the pH dependence of protein stability and function have been performed on a large array of different systems using NMR approaches.[6−8] However, in practice applications have focused on relatively small proteins, with the 20S CP well over an order of magnitude larger than molecules that have been studied in the past.

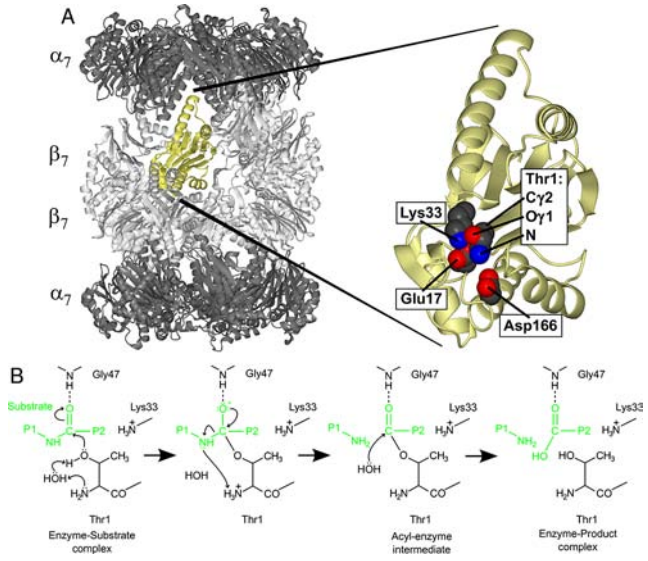


**Figure 1.** (A) Ribbon diagram representation of the *T. acidophilum* 20S CP (1YA7),[23] with the heptameric $\alpha$ ($\beta$) rings in black (gray). A pair of $\beta$ subunits have been removed to provide a better view of the "yellow" $\beta$ subunit that is highlighted to the right, showing the arrangement of ionizable residues at or near the active site. (B) Proposed reaction scheme for 20S CP-catalyzed peptide bond hydrolysis. Residues from the CP are in black, while the substrate is in green. Details are given in the text.

The development of isotope labeling strategies whereby very high molecular weight proteins are methyl-protonated in an otherwise highly deuterated background, coupled with the use of NMR experiments that preserve magnetization from methyl group probes, has significantly increased the scope of NMR

**Received:** March 27, 2013
**Published:** May 2, 2013

  

applications.[9] It has now become possible to undertake quantitative NMR studies on some protein systems with aggregate molecular weights up to 1 MDa, including the 20S proteasome CP and its complexes with regulatory particles.[10−12] Of particular interest for the present study is the fact that a protocol for preparing Thr in a form that is methyl-protonated ($^{13}CH_3$) and deuterated at the C$\alpha$ and C$\beta$ positions has become available.[13] Precursors generated in this manner can be added to protein expression media to generate highly deuterated molecules with protonated methyl groups at Thr positions, complementing previously described schemes for obtaining protonated methyl groups at side chains of Ala, Ile, Leu, Val, and Met residues.[14−19] Here we have exploited this new technology and used the methyl group of Thr1 as a probe of the ionization state of the amino terminus, establishing that the Thr1 amino group is deprotonated in the substrate-free form of the enzyme at neutral pH, in support of the model for proteasome catalysis.

A tentative mechanism for substrate hydrolysis, based on site-directed mutagenesis[20−22] and X-ray crystallography,[3,4] is illustrated in Figure 1B. Transfer of Thr1 H$\gamma$1 to the assumed neutral amino-terminal group (see below) may be facilitated by a crystallographically observed water that is close to both Thr1 O$\gamma$1 and N atoms. Subsequent nucleophilic attack of the substrate peptide bond undergoing hydrolysis by Thr1 O$\gamma$1 results in the formation of a tetrahedral oxyanion that is stabilized by the backbone amide of Gly47.[4] As the oxyanion collapses, the peptide bond of the substrate is cleaved, leaving an acyl−enzyme intermediate that is thought to resemble the active site of numerous complexes of the proteasome with bound covalent inhibitors.[1,4] The water molecule mentioned above plays a critical role in the next step, where it is assumed to attack the substrate−enzyme ester, producing a second product peptide and regenerating the enzyme. Thus, the available data suggest that catalysis is mediated exclusively by Thr1 and that the role of Lys33, Glu17, and Asp166 is to provide the appropriate electrostatic environment to facilitate the reaction.

As described above, central to the first step in the reaction scheme of Figure 1B is that Thr1 is neutral, so as to serve as a catalytic base. In order to test this assumption, we began by preparing samples of highly deuterated proteasome labeled as $^{13}CH_3$-Thr using either a commercially available U-[$^{13}$C,$^{1}$H]-Thr precursor or [$\alpha$-$^{2}$H;$\beta$-$^{2}$H;$\gamma$-$^{13}$C]-Thr that has been produced in-house.[13] $^{13}$C−$^{1}$H HMQC correlation maps that benefit from a methyl-TROSY effect[24] are illustrated in Figure 2A,B, showing clear improvements when deuteration extends to the $\alpha$ and $\beta$ positions of the residue. For example, correlations from all 15 Thr methyl groups are observed in the HMQC spectrum of [$\alpha$-$^{2}$H;$\beta$-$^{2}$H;$\gamma$-$^{13}$C]-Thr proteasome (Figure 2B), while a much smaller number of peaks are visible in the data set measured on the sample prepared as U-[$^{13}$C,$^{1}$H]-Thr (Figure 2A). Spectra from samples generated with the [$\alpha$-$^{2}$H;$\beta$-$^{2}$H;$\gamma$-$^{13}$C]-Thr label were analyzed in what follows. Assignments for many of the Thr peaks could be obtained from NOEs connecting the methyl groups of previously assigned Ile, Leu, and Val residues[12] to Thr, interpreted on the basis of the available X-ray structural model of the complex.[23] Correlations from Thr1, Thr3, Thr16, and Thr44, with all four residues localized to a single central $\beta$-sandwich, could not be assigned unambiguously via NOE patterns. In order to obtain the assignment of Thr1, we prepared a pair of 20S CP samples with (i) T1C and (ii) T3S, T16S, and T44S mutations and

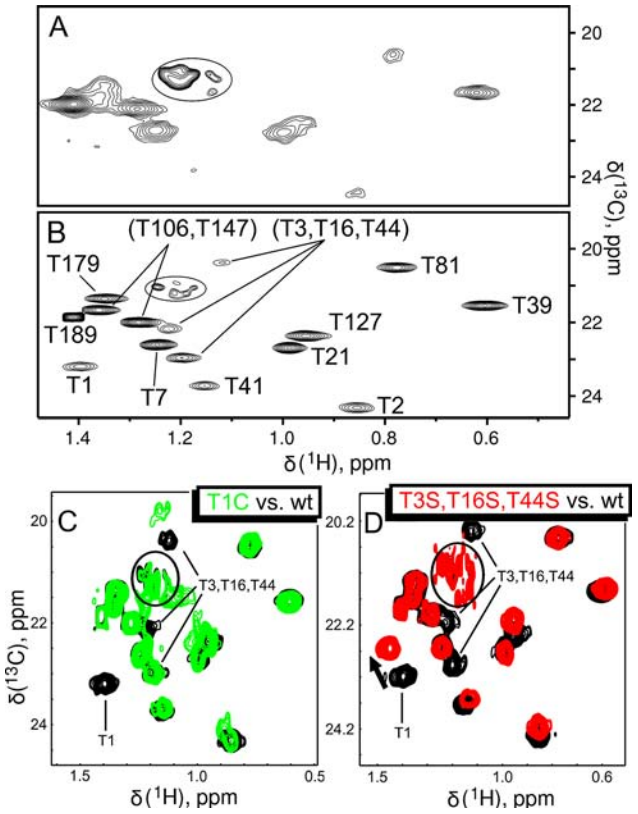


**Figure 2.** $^{13}$C−$^{1}$H HMQC correlation maps of the Thr region of the 20S CP, 18.8 T, 70 °C, with labeling restricted to the $\beta$-rings only. Labeling was accomplished by adding U-[$^{13}$C,$^{1}$H]-Thr (A) or [$\alpha$-$^{2}$H;$\beta$-$^{2}$H;$\gamma$-$^{13}$C]-Thr label (B) prior to the induction of protein overexpression, as described previously.[13] Assignments of the 15 Thr cross-peaks are as indicated. (C,D) Assignment of Thr1 has been achieved via mutagenesis, exploiting T1C and T3S, T16S, T44S 20S CP samples, as described in the text. Spectra of the wild-type (wt) protein are shown in black. Peaks from a protein species that slowly increases in concentration over time are indicated by the circles.

compared their NMR spectra. The peak resonating at (23.20 ppm, 1.40 ppm) in the $^{13}$C and $^{1}$H dimensions is eliminated in T1C, Figure 2C, while it is still present at a slightly shifted location in the triple mutant, Figure 2D. This cross-peak could therefore be assigned to the $\gamma$2 methyl of catalytic residue Thr1. In total, 10 of the 15 Thr correlations have been assigned. Of the remaining five peaks, two are very strong (Thr106 and Thr147), but neither of the Thr residues from which they are derived is proximal to a methyl-containing group in the structure, so no NOEs are observed. The remaining three weak correlations have been assigned to T3, T16, and T44 (although the identity of each peak is not known) on the basis of the Thr-to-Ser substitutions described above.

After assignment of the Thr1 methyl group, a titration over a pH range extending from 5 to 10 was performed. With the exception of Thr1, the positions of all of the remaining Thr correlations changed little; by contrast, Thr1 shifted by close to 1 ppm in $^{13}$C and 0.14 ppm in $^{1}$H, as might be expected if the terminal amino group titrates within this range, Figure S1. Measured chemical shifts fit only poorly to a simple Henderson−Hasselbalch equation assuming a single p$K_A$ value, Figure S2. We therefore interpreted our data using a "spectroscopically coupled" model[8] involving a pair of protonation events that are thermodynamically independent


dx.doi.org/10.1021/ja403091c | J. Am. Chem. Soc. 2013, 135, 9259−9262

but where the chemical shifts of the reporter nuclei depend on the ionization state of both titratable moieties (see Supporting Information). Such a scheme is indicated in Figure 3A with the

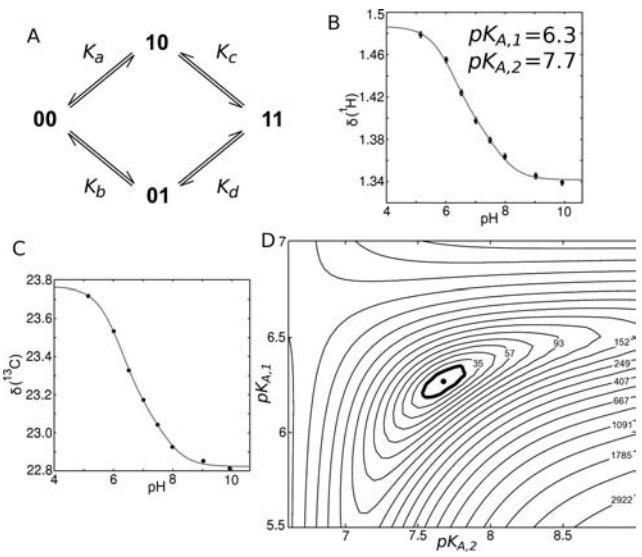


**Figure 3.** Extraction of p$K_A$ values from the titration data of Thr1. (A) Model involving two titratable groups, where 0 and 1 indicate deprotonated and protonated sites, respectively. For example, 00 indicates that both sites are in the deprotonated state. In the most general case, three unique p$K_A$ values are required, with the fourth obtained from the relation $K_aK_c = K_bK_d$. Chemical shift profiles have been fit simultaneously to a model of two microscopic p$K_A$ values that derive from sites that are non-interacting, $K_a = K_d = K_{A,1}$ and $K_b = K_c = K_{A,2}$. (B,C) Best-fit curves (solid lines) from simultaneous fits of $^1$H (B) and $^{13}$C (C) chemical shift titration data (circles). Error bars are within the sizes of the circles denoting measured shifts. (D) Contour plot of the $\chi^2$ surface from the fit, showing the global minimum with a dot ($\chi^2_{MIN}$ = 21.0; 8 degrees of freedom) and the 95% confidence area with a thick contour ($\chi^2 = \chi^2_{MIN} + 6.18$).[25] Contours are spaced on a logarithmic scale, with $\chi^2$ values indicated on every second contour.

microscopic dissociation constants, $K_i$ ($i \in \{a,b,c,d\}$), related as $K_a = K_d = K_{A,1}$ and $K_b = K_c = K_{A,2}$. Initial independent fits of the $^1$H and $^{13}$C chemical shift titration data led to very similar p$K_A$ values (Figure S2), justifying simultaneous analysis involving both sets of data. p$K_{A,1}$ and p$K_{A,2}$ values of 6.3 and 7.7 were obtained, Figure 3B,C, with the 95% confidence regions ranging from 6.18 to 6.35 and from 7.53 to 7.83, Figure 3D.

As has been described previously, any titration curve based on two ionization events can be fit by a general macroscopic binding model with two p$K_A$ values and three chemical shifts,[8] irrespective of the underlying microscopic mechanism giving rise to the titration profile. The two extracted p$K_A$ values from fits using the macroscopic binding model[8] do not necessarily have an interpretation in terms of a microscopic process. However, in the case where the obtained p$K_A$ values from a fit to a microscopic model are significantly different ($|pK_{A,1} - pK_{A,2}| \geq 1$), as in the present situation, both macroscopic and non-cooperative microscopic models reduce to a model that assumes independent sequential protonation events.[8] Indeed, fitting our data to a macroscopic model produced p$K_A$ values within 0.02 unit of the microscopic values and an identical $\chi^2$ value. While our data appears to be well described by a microscopic model with independent p$K_{A,1}$ and p$K_{A,2}$ values of 6.3 and 7.7, it is possible that the underlying molecular details are more complex, with the two ionization events thermodynamically coupled.[8] In this case three independent p$K_A$ values are required to describe such a system using a microscopic model, with the fourth obtained by summing over the thermodynamic cycle, Figure 3A (or equivalently 2 p$K_A$ values and one cooperativity factor $\alpha$, see Supporting Information). Although the NMR titration data can be well fitted to a model with two independent p$K_A$ values, p$K_{A,1}$ and p$K_{A,2}$, a relationship can be derived to describe the four microscopic p$K_A$ values of the general scheme of Figure 3A in terms of p$K_{A,1}$, p$K_{A,2}$, and $\alpha$, as discussed in the Supporting Information. For the most extreme case of cooperativity compatible with our titration data, we find that both p$K_c$ and p$K_d$ converge to 6.6, with $\alpha$ = 0.15. Thus, starting from a fully protonated state (1,1 in the scheme of Figure 3A), the p$K_A$ corresponding to the release of the first proton is calculated to be 6.6, as opposed to 6.3 that is obtained from a model that does not assume cooperativity ($\alpha$ = 1), Figure S3. Thus, independent of the model used to fit the data, the overall picture, as described below, remains similar.

What is the nature of the two titrating groups that we observe? Figure 1B shows that there are four titratable moieties (one amino group from each of Thr1 and Lys 33 and two carboxylates, Glu17 and Asp166) that are proximal to the reporter Thr1 $\gamma$2 methyl group. The p$K_A$ values reported here (6.3 and 7.7) have not been corrected to take into account that the titration was performed in a 99% $D_2O$ solution, so the pH values measured are approximately 0.4 unit lower than for the corresponding $H_2O$ solution. Even with the correction, the p$K_A$ values do not precisely match reported values for unperturbed amines (8.0 and 10.8),[26] although they are significantly closer to what is expected for amines than for carboxylates (4.1).[26] Thus, we assign the p$K_A$ values of 6.3 and 7.7 to the N-terminal amine (Thr1) and the Lys33 amino group, respectively. In order to confirm the assigned p$K_A$ values, we have prepared 20S CP with an Asp-to-Asn substitution at position 166 in the $\beta$ subunits. Mutants with Asp166 substitutions are no longer functional,[22] so that the prosequence that preceeds Thr1, and that is normally cleaved by active 20S CP in the final step of proteasome assembly,[22] remains attached. In this manner the amino group of Thr1 is converted to an amide and can no longer titrate. If our assignments are correct, then the prediction is that the Thr 1 methyl group would no longer titrate in the pH range 6−7. Comparison of the titration profiles of the wild-type 20S CP (Figure 4A) and the Asp166Asn mutant (B), focusing on Thr 1, shows that this is indeed the case. The interplay between the N-terminus, Lys33, Glu17, and Asp166, together with hydrogen-bonding effects from nearby backbone and side-chain atoms, must therefore

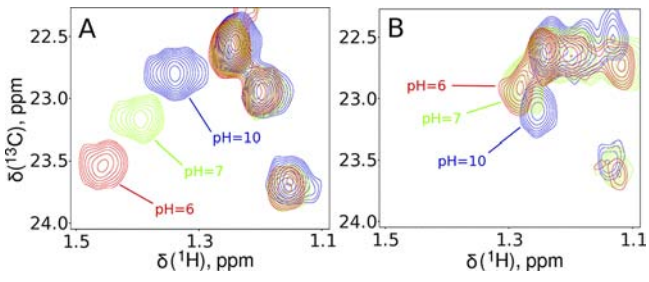


**Figure 4.** Superposition of $^{13}$C−$^1$H HMQC correlation maps of wild-type (A) and Asp166Asn (B) 20S CP focusing on Thr1 and recorded at pH 6 (red), 7 (green), and 10 (blue), 18.8 T, 70 °C.


dx.doi.org/10.1021/ja403091c | J. Am. Chem. Soc. 2013, 135, 9259−9262

account for the deviations in $pK_A$ values from those corresponding to free amino acids.

Our results are consistent with and lend support to the proposed mechanism of substrate hydrolysis (Figure 1B), since they imply that the N-terminal amine exists largely in a deprotonated state at neutral pH. This amino group would thus be able to function as a base, accepting a hydrogen from the Thr1 hydroxyl group, resulting in efficient catalysis in the pH range 6−9, where maximum activity of the *T. acidophilum* 20S CP has been observed experimentally.[3] Interestingly, our data supporting the fact that the catalytic base is neutral in the substrate-free form of the proteasome are consistent with studies on the catalytic triad histidine in serine proteases such as chymotrypsin. NMR pH titrations of chymotrypsin bound to a transition-state analogue establish a shift in $pK_A$ of the histidine from 7.5 in the free enzyme to 10.8−12.0 in the complex.[27] The elevated histidine $pK_A$ in complex with substrate would make it better able to retain the proton that is removed from the catalytic serine, facilitating formation of a Ser alkoxide anion that is critical to catalysis. Recent studies of complexes of fluorinated inhibitors and the 20S CP suggest that a similar mechanism may be operative for the proteasome as well,[28] with the amino terminus of Thr1 functioning as a catalytic base whose $pK_A$ increases between substrate-free and bound states. This, in turn, leads to deprotonation of the Thr1 hydroxyl in a more efficient manner.

In summary, we report here a pH study addressing the first stage of the catalytic mechanism of the 20S CP proteasome. Using a highly deuterated 20S CP sample with Thr labeled as [$\alpha$-$^2$H;$\beta$-$^2$H;$\gamma$-$^{13}$C] in concert with methyl-TROSY NMR spectroscopy, high-quality $^{13}$C−$^1$H spectra were obtained so that the pH dependence of Thr1 methyl $^{13}$C and $^1$H chemical shifts could be quantified. The fitted $pK_A$ value for the Thr1 amino group (6.3) indicates that the terminus is neutral over the pH optimum range, so that it can function as an efficient catalytic base in the first step of the hydrolysis reaction, Figure 1B. Given that the proteasome is a multi-billion dollar drug target in the fight against certain classes of cancers and neurodegenerative disorders,[29,30] an understanding of its mechanism is critical. This study provides an important step in that direction.

## ■ ASSOCIATED CONTENT

### Supporting Information

Discussion of titration models and methods; figures showing titration spectra, fits of titration data assuming a single titrating group, and variation of $pK_i$ ($i \in \{a,b,c,d\}$) values with cooperativity. This material is available free of charge via the Internet at http://pubs.acs.org

## ■ AUTHOR INFORMATION

### Corresponding Author

avelyvis@pound.med.utoronto.ca; kay@pound.med.utoronto

### Notes

The authors declare no competing financial interest.

## ■ ACKNOWLEDGMENTS

We thank Prof. Julie Forman-Kay (Hospital for Sick Children, Toronto) for providing laboratory facilities for protein purification. This work was supported by a grant from the Natural Sciences and Engineering Research Council of Canada. L.E.K. holds a Canada Research Chair in Biochemistry.

## ■ REFERENCES

(1) Marques, A. J.; Palanimurugan, R.; Matias, A. C.; Ramos, P. C.; Dohmen, R. J. *Chem. Rev.* **2009**, *109*, 1509.
(2) Zwickl, P.; Kleinz, J.; Baumeister, W. *Nat. Struct. Biol.* **1994**, *1*, 765.
(3) Löwe, J.; Stock, D.; Jap, B.; Zwickl, P.; Baumeister, W.; Huber, R. *Science* **1995**, *268*, 533.
(4) Groll, M.; Ditzel, L.; Löwe, J.; Stock, D.; Bochtler, M.; Bartunik, H. D.; Huber, R. *Nature* **1997**, *386*, 463.
(5) Dahlmann, B.; Kuehn, L.; Grziwa, A.; Zwickl, P.; Baumeister, W. *Eur. J. Biochem.* **1992**, *208*, 789.
(6) Forman-Kay, J. D.; Clore, G. M.; Gronenborn, A. M. *Biochemistry* **1992**, *31*, 3442.
(7) Pelton, J. G.; Torchia, D. A.; Meadow, N. D.; Roseman, S. *Protein Sci.* **1993**, *2*, 543.
(8) McIntosh, L. P.; Naito, D.; Baturin, S. J.; Okon, M.; Joshi, M. D.; Nielsen, J. E. *J. Biomol. NMR* **2011**, *51*, 5.
(9) Ruschak, A. M.; Kay, L. E. *J. Biomol. NMR* **2010**, *46*, 75.
(10) Sprangers, R.; Kay, L. E. *Nature* **2007**, *445*, 618.
(11) Religa, T. L.; Sprangers, R.; Kay, L. E. *Science* **2010**, *328*, 98.
(12) Ruschak, A. M.; Kay, L. E. *Proc. Natl. Acad. Sci. U.S.A.* **2012**, *109*, E3454.
(13) Velyvis, A.; Ruschak, A. M.; Kay, L. E. *PLoS One* **2012**, *7*, e43725.
(14) Tugarinov, V.; Kay, L. E. *J. Biomol. NMR* **2004**, *28*, 165.
(15) Isaacson, R. L.; Simpson, P. J.; Liu, M.; Cota, E.; Zhang, X.; Freemont, P.; Matthews, S. *J. Am. Chem. Soc.* **2007**, *129*, 15428.
(16) Ayala, I.; Sounier, R.; Usé, N.; Gans, P.; Boisbouvier, J. *J. Biomol. NMR* **2009**, *43*, 111.
(17) Gans, P.; Hamelin, O.; Sounier, R.; Ayala, I.; Durá, M. A.; Amero, C. D.; Noirclerc-Savoye, M.; Franzetti, B.; Plevin, M. J.; Boisbouvier, J. *Angew. Chem., Int. Ed.* **2010**, *49*, 1958.
(18) Gelis, I.; Bonvin, A. M. J. J.; Keramisanou, D.; Koukaki, M.; Gouridis, G.; Karamanou, S.; Economou, A.; Kalodimos, C. G. *Cell* **2007**, *131*, 756.
(19) Fischer, M.; Kloiber, K.; Häusler, J.; Ledolter, K.; Konrat, R.; Schmid, W. *Chembiochem* **2007**, *8*, 610.
(20) Seemüller, E.; Lupas, A.; Zühl, F.; Zwickl, P.; Baumeister, W. *FEBS Lett.* **1995**, *359*, 173.
(21) Seemüller, E.; Lupas, A.; Stock, D.; Löwe, J.; Huber, R.; Baumeister, W. *Science* **1995**, *268*, 579.
(22) Seemuller, E.; Lupas, A.; Baumeister, W. *Nature* **1996**, *382*, 468.
(23) Förster, A.; Masters, E. I.; Whitby, F. G.; Robinson, H.; Hill, C. P. *Mol. Cell* **2005**, *18*, 589.
(24) Tugarinov, V.; Hwang, P. M.; Ollerenshaw, J. E.; Kay, L. E. *J. Am. Chem. Soc.* **2003**, *125*, 10420.
(25) Press, W. H.; Teukolsky, S. A.; Vetterling, W. T.; Flannery, B. P. *Numerical Recipes*, 3rd ed.; Cambridge University Press: Cambridge, 2007.
(26) Berg, J. M.; Tymoczko, J. L.; Stryer, L. *Biochemistry*, 6th ed.; W. H. Freeman and Co.: New York, 2007.
(27) Cassidy, C. S.; Lin, J.; Frey, P. A. *Biochemistry* **1997**, *36*, 4576.
(28) Groll, M.; McArthur, K. A.; Macherla, V. R.; Manam, R. R.; Potts, B. C. *J. Med. Chem.* **2009**, *52*, 5420.
(29) Goldberg, A. L. *J. Cell Biol.* **2012**, *199*, 583.
(30) Ying, Z.; Wang, H.; Wang, G. *Curr. Pharm. Des.* **2013**, *19*, 3305.